

On the possibility of high-level transient coronal mass ejection–induced ionospheric current coupling to electric power grids

Jamesina J. Simpson¹

Received 11 May 2011; revised 22 August 2011; accepted 24 August 2011; published 9 November 2011.

[1] Short-time (<10 s) ionospheric current fluctuations are hypothesized to occur due to a coronal mass ejection that can induce high-level transient voltages on long overhead power transmission lines. This hypothesis is first supported by reviewing published literature and recent magnetometer measurements, both of which indicate the existence of such rapid ionospheric current fluctuations. Then results are reported of a new full-vector three-dimensional Maxwell's equations finite-difference time-domain (FDTD) model of the global Earth-ionosphere system during a solar storm. This model naturally treats transient electromagnetic fields and waves unlike previous quasi-DC steady state or sinusoidal steady state analyses. Furthermore, this model accounts for the geometrical and electrical properties of the entire global Earth-ionosphere system, including details of the global topography and bathymetry, rather than focusing upon a particular continental region as for previous analyses. The FDTD modeling results provide new and useful information, such as that the lithosphere conductivity has almost no impact on the induced transient (short timescale) surface geoelectric fields resulting from capacitive or electric field coupling mechanisms. This is counter to the previously analyzed magnetic field coupling mechanisms involving the (long timescale) induction of geomagnetically induced currents, which heavily depend on the lithosphere conductivity structure. The modeling results presented herein are sufficiently significant to warrant measurements of rapid ionospheric current fluctuations at timescales much shorter than considered at present, even less than 1 s.

Citation: Simpson, J. J. (2011), On the possibility of high-level transient coronal mass ejection–induced ionospheric current coupling to electric power grids, *J. Geophys. Res.*, 116, A11308, doi:10.1029/2011JA016830.

1. Introduction

[2] In March 1989, a coronal mass ejection (CME) caused the HydroQuebec power grid to fail for 9 h, leaving 6 million customers without electricity and having an overall economic cost in the millions of dollars [Bolduc, 2002]. The *National Research Council of the National Academies* [2008] estimated that a CME having the intensity of the severe 1859 event could have an economic cost in the trillions of dollars and impose a societal recovery time of 4–10 years.

[3] The literature provides extensive evidence for, and discussion of, the hazards posed by CME-generated geomagnetically induced currents (GICs) on the operation of power grids [see, e.g., Kappenman, 2005, 2006; Pulkkinen *et al.*, 2010]. Currents flowing within the lithosphere are essentially images of currents flowing within the ionosphere. Since the early 1980s, observatories have collected digital geomagnetic field data with a temporal resolution in

the order of ~1 min which can be used to monitor GICs. During the 1990s, the Electric Power Research Institute (EPRI) established the SUNBURST monitoring network for GICs [Lesher *et al.*, 1994].

[4] In addition to measurements, numerical modeling has been carried out to study GICs under varying solar storm conditions. For example, Shao *et al.* [2002] employed a magnetohydrodynamic (MHD) ionosphere model with the Biot-Savart Law (i.e., a magnetostatic approximation) to project magnetic fields onto the Earth's surface. Pulkkinen *et al.* [2007] applied an MHD model along with the methodology of Raeder *et al.* [2001] to map ionospheric currents to ~100 km altitude, and then calculate the surface magnetic fields via complex image theory. Shepherd and Shubitidze [2003] made similar calculations using the method of auxiliary sources. More recently, Viljanen *et al.* [2006] measured magnetic fields at Earth's surface and then utilized a plane wave theory to calculate the corresponding surface geoelectric fields, which in turn were used to estimate GICs.

[5] Note that these electromagnetic field analyses employ quasi-DC and sinusoidal steady state (phasor domain) mathematical formulations which are suitable for evaluating GICs that vary over timescales of tens of seconds. There

¹Electrical and Computer Engineering Department, University of New Mexico, Albuquerque, New Mexico, USA.

appears to be no published literature regarding the measurement, analysis, or numerical modeling of solar storm-generated transient electromagnetic phenomena having characteristic timescales below 10 s (with the exception of older publications involving analog measurements such as *Hessler and Wescott* [1959] and *Sanders* [1961]).

[6] In this paper, the possibility is proposed that precisely such short-time transient electromagnetic phenomena generated by an historically severe CME can induce impulses exceeding 10 kV on long overhead power transmission lines. That is, for example, assuming for simplicity an induced, approximately uniform geoelectric field of 100 V/km along the length of one power line whose length is 100 km, this would produce a voltage of 10 kV in that power line. Further, a complete picture of the transient electrodynamics associated with CMEs and their impact upon power grids requires a time domain, fully vectorial Maxwell's equations model of the entire global Earth-ionosphere system under disturbed conditions. Reported herein is what is believed to be the first such model.

[7] Specifically, the three-dimensional (3-D) finite-difference time-domain (FDTD) method [*Taflove and Hagness*, 2005] is applied to model the electrodynamics of the complete global Earth-ionosphere system [*Simpson*, 2009; *Simpson and Taflove*, 2007] during the 29–31 October 2003 “Halloween storm” [*Kotobi et al.*, 2011]. For this study, the global FDTD Earth-ionosphere model of *Simpson and Taflove* [2004] is employed, which has been previously applied toward investigating remote sensing of ionospheric anomalies [*Simpson and Taflove*, 2006a] and underground oil fields [*Simpson and Taflove*, 2006b], and toward calculating the temporal and spectral signatures of hypothetical extremely low-frequency earthquake precursors [*Simpson and Taflove*, 2005; *Simpson*, 2009].

[8] The FDTD model utilized in the present study has the following robust attributes.

[9] 1. It computes electromagnetic wave propagation dynamics within the entire global Earth-ionosphere cavity via the complete Maxwell's equations (including displacement currents) on a 3-D grid having a spatial resolution measured in kilometers.

[10] 2. The FDTD model includes at each electric (E) field vector component the local dielectric permittivity and electrical conductivity. Hence, the spatial geometry and electrical properties of all of the matter within the global Earth-ionosphere cavity (lithosphere constituents, ocean water, lossless air, and ionospheric plasma layers) are mapped into the 3-D FDTD grid with a kilometer-scale spatial resolution. For example, lithosphere regions of highly resistive igneous rock where power systems are more vulnerable to GICs [*Kappenman et al.*, 1997] are incorporated into the model.

[11] 3. The FDTD model incorporates in the variability of the ionospheric layering and height with day and night, and also incorporates 3-D spatially variable ionospheric current directions and magnitudes.

[12] 4. In addition to computing the time waveforms of the electric and magnetic fields anywhere within the model, the spectral behavior of these fields at selected grid points can be obtained over a wide range of frequencies during a single FDTD modeling run via a concurrent discrete Fourier

transformation of the field versus time waveform at each selected monitor point.

[13] Note that the FDTD model of the global Earth-ionosphere system utilized in the present study was previously validated by comparing its calculations of long-distance propagation of extremely low-frequency electromagnetic waves about the Earth with the measured and analytical data reported in the work of *Bannister* [1985]. Excellent agreement was obtained [*Simpson and Taflove*, 2004].

2. Existence of Ionospheric Currents Fluctuating Over Characteristic Times <20 s

[14] Published and measurement results indicate the existence of rapidly varying (characteristic times <20 s) electromagnetic fields at Earth's surface during a solar storm, generated by correspondingly rapid ionospheric current fluctuations. Some examples will now be reviewed.

[15] First, Figure 1 shows the measured surface northward component magnetic field recorded at 1 s intervals at Qeqertarsuaq, Greenland (GDH station) on 15 January 2011 as provided by the National Space Institute at the Technical University of Denmark. Magnetometers having the capability to digitally record the surface magnetic field at intervals of <10 s have only more recently been taken advantage of for space weather applications. For example, despite the availability of 1 s magnetometer data since about 2005 through the National Space Institute, from 2005 until 2011 this 1 s measured data were always filtered to a 20 s sampling rate before being checked and analyzed by the National Space Institute (C. Stolle, private communication, 2011). Hence, the example magnetic field data shown in this paper are from a recent 2011 measurement for which the complete 1 s available data have been utilized and checked. Note that as a result, the January 2011 measurement data presented here correspond to a solar minimum and during a time period of only small-scale CMEs.

[16] Indeed, to date, magnetometer data at 10–20 s intervals have been sufficient because the primary focus of studies relating to CME effects and hazards on the Earth-ionosphere system has only been with regards to long-timescale effects. To the author's knowledge, no magnetic field measurements at sampling rates of less than 1 s are yet available for studying the effects of space weather on Earth, and measurements at 1 s are only starting to perhaps be utilized.

[17] Examining Figure 1, the rapid decline of the magnetic field seen to start around 04:40:00 UT is due to a relatively small-scale CME. In Figure 2, a close-up view of the data shown in Figure 1 is illustrated, focusing on a time period during this rapid decline of the magnetic field owing to the CME. Specifically, in Figure 2, a total of 20 s (resulting in 21 data points) is shown starting at 04:48:00 UT on 15 January 2011. A simple linear interpolation between data points is assumed here just to illustrate the rapid change in the measurement data between 4:48:08 and 4:48:09. Indeed, the choppy behavior of the measurement data at 4:48:08–4:48:09, indicates that the 1 s sampling magnetometer is not capturing the complete behavior of the magnetic field, and fluctuations of lengths <1 s must be occurring between the sampling times. The 1 s sampled magnetic field time

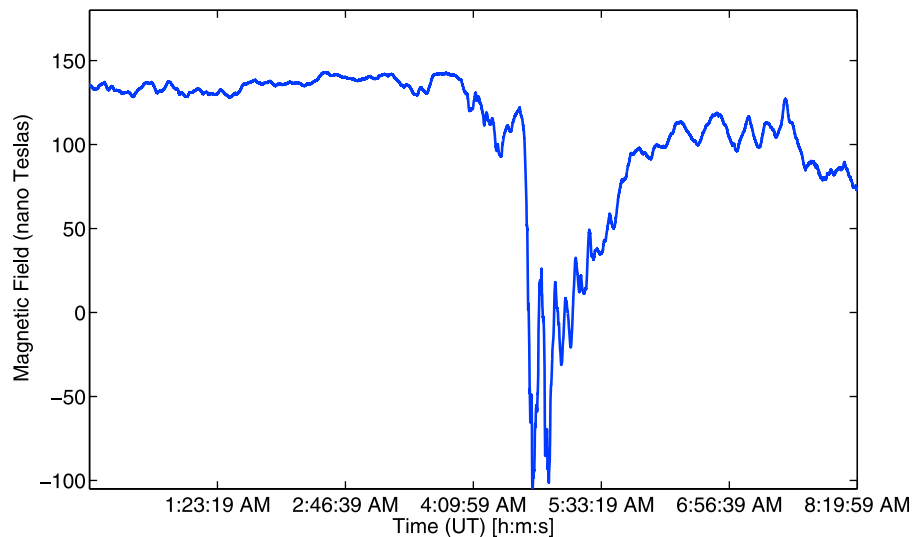


Figure 1. Measured surface north component magnetic field recorded at 1 s intervals at Qeqertarsuaq, Greenland (GDH station), on 15 January 2011. From C. Stolle (private communication, 2011).

waveform of Figure 2 is therefore an aliased and low-pass filtered version of the actual time waveform.

[18] Then, a natural question to ask is, how might the magnetic field look if it were sampled at a rate even faster than 1 s? Would there be even more rapid changes in the magnetic field over certain short time periods? Could some of these changes be considered significant enough to yield hazards to power grids? Because only long-timescale (>10 s) CME effects on the Earth have been studied to date, these questions remain unanswered, especially for extreme CMEs. But, the results of this paper indicate that such studies to obtain the answers to these questions would be important to conduct.

[19] The potential occurrence of rapid magnetic field fluctuations having lengths <10 s, as indicated by Figure 2,

is given a more quantitative basis by the statistical study of Figure 3, which was taken from *Pulkkinen et al.* [2006]. Figure 3 depicts the probability distribution of magnetic field pulse lengths for the “Halloween” storms of October 2003. In Figure 3, only pulses having time rates of change >1 nT/s and lengths >20 s were included in the data record (indeed only long timescales are again considered), yielding a total of 2398 pulses. Subject to these limits, observe in Figure 3 a clear trend wherein shorter pulse lengths have a progressively increased probability of occurrence. There is no indication of a reversal of this trend for pulse lengths <20 s, although short-timescale studies must be performed to establish the actual behavior of this curve for <20 s. Further, other storms should also be analyzed for magnetic field pulse length probabilities. In fact, considering the

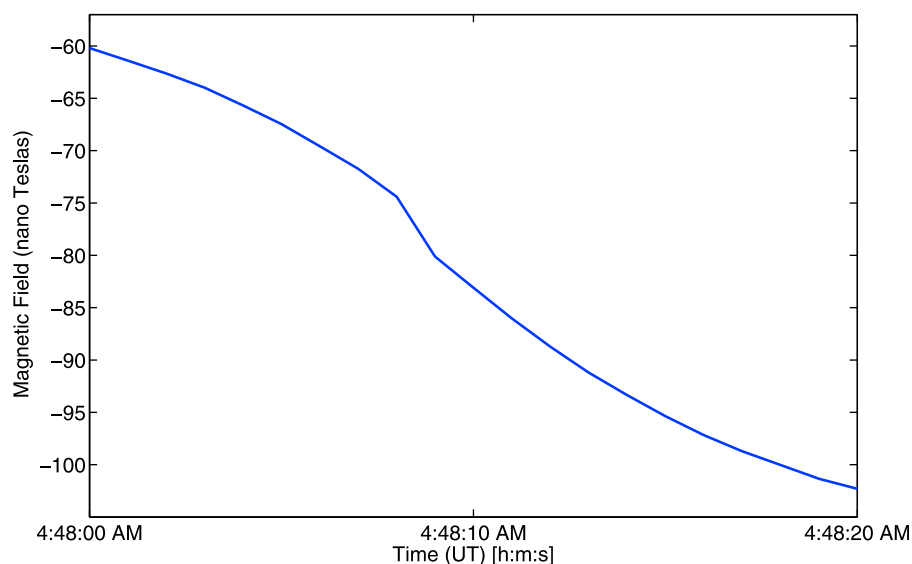


Figure 2. Close-up of Figure 1 illustrating the behavior of the measured surface north component magnetic field at Qeqertarsuaq, Greenland (GDH station), on 15 January 2011 over 20 s starting at 04:48:00. The measured data are plotted at 1 s time increments. From C. Stolle (private communication, 2011).

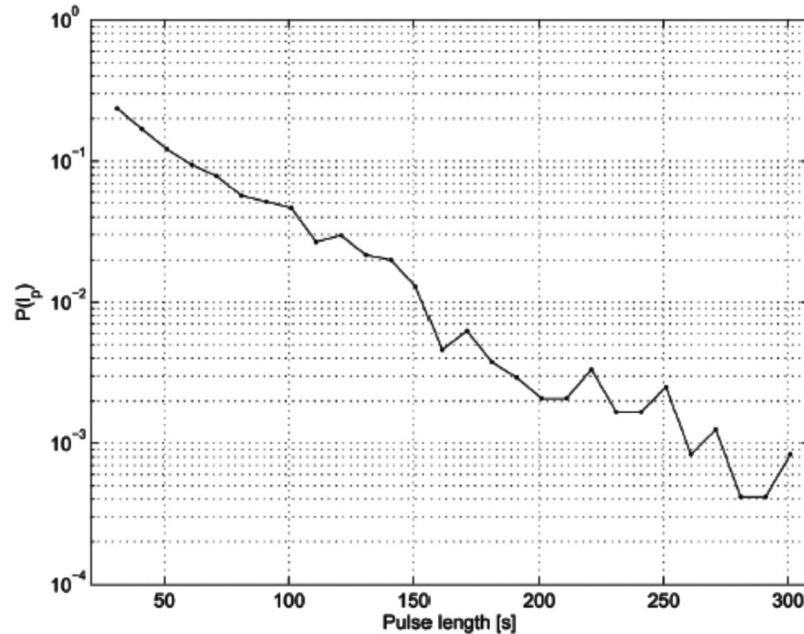


Figure 3. Probability distribution of magnetic field pulse lengths for the Halloween storms of October 2003. From *Pulkkinen et al.* [2006].

research and conclusions of this paper this should be considered future proposed work.

[20] Finally, solar storm-induced geoelectric fields fluctuating over characteristic times as short as 1 s were measured using analog equipment in Alaska [*Hessler and Wescott*, 1959; *Sanders*, 1961]. The latter article is discussed further in section 3. The 1 s fluctuation regime is precisely the one of interest in the present computational modeling study.

3. Need for a More Comprehensive Electrodynamics Model

[21] In early work, *Sanders* [1961] proposed two mechanisms (or approaches) for calculating the surface electromagnetic fields induced by a solar storm: (1) a (quasi)-DC magnetic field generated according to the Biot-Savart Law; and (2) an electric field generated by the negative time derivative of the magnetic field according to Faraday's Law. However, *Sanders* [1961] stated that "neither hypothesis is entirely satisfactory" and furthermore "no satisfactory explanation of the generation of Earth currents is offered by current ionospheric and magnetic theories."

[22] In more recent literature [see, e.g., *Viljanen et al.*, 2006], an alternative mechanism (approach) is proposed wherein (3) the electric and magnetic fields are two components of a common plane wave, and are therefore linearly scaled by the wave impedance. This plane wave method has proved to be very useful in analyzing long-timescale electrodynamic effects caused by CMEs. However, it is incapable of accurately calculating the short-timescale effects and surface geoelectric and magnetic fields, which would require a full-vector time domain Maxwell's equations solution involving both Ampere's and Faraday's Laws and global calculations. The FDTD model described in section 4

provides such full-vector Maxwell's equations calculations. This need for a complete Maxwell's equations solution is exemplified by the fact that surface geoelectric and magnetic field results obtained from the plane wave method are known to depend heavily on the underlying ground conductivity structure [*Pulkkinen et al.*, 2007]. In the transient, Maxwell's equations results of this paper, however, it is found that the short-timescale geoelectric fields are almost identical for different ground conductivity models. This is highlighted further in section 5.

[23] The author agrees with the assessment of *Sanders* [1961], and furthermore asserts that published results and measurements as discussed in section 2 cast doubt on the ability of the mechanism of *Viljanen et al.* [2006] to provide a comprehensive and accurate calculation of the fields at all locations and time spans of interest (transient, in addition to the long timescales) during storms. Specifically, consider *Sanders* [1961, Figure 6], which for convenience is reprinted here as Figure 4. Figure 4 (top) and Figure 4 (bottom) show the surface geoelectric and magnetic fields during the 31 March to 3 April 1960 storm, respectively. The wirelines from which the geoelectric fields were obtained were located at $\sim 41^\circ\text{N}$ latitude, 32° geomagnetic, very close to Iowa City (42°N , 33° geomagnetic) where the magnetic fields were recorded. From 12:00 to 24:00 UT, we see that the geoelectric fields oscillate significantly more rapidly than the corresponding magnetic field, and furthermore the upward trend in the magnetic field is not reflected in the geoelectric field. In sum, the geoelectric and magnetic field behaviors are essentially uncorrelated during this time span, a fact that is unexplainable by invoking any or all of the three hypothesized mechanisms noted above. On the other hand, it is important to mention that there are also many sources of electric fields (thunderstorms, for example), which could also lead to a lack of correlation between the

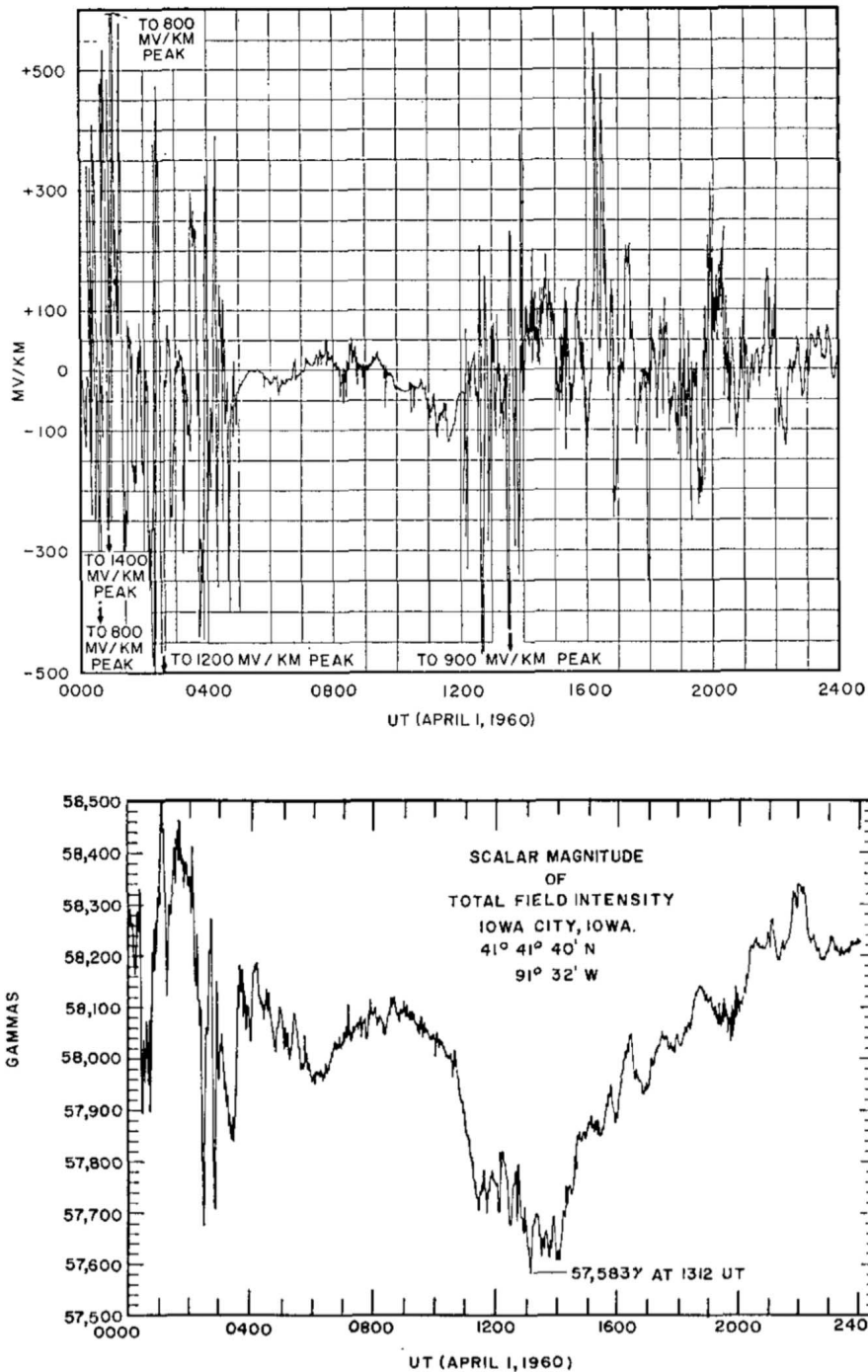


Figure 4. Surface electromagnetic fields during the 31 March to 3 April 1960 solar storm. (top) Tellurigram reconstructed from wireline geoelectric field data. (bottom) Magnetograph of the geomagnetic fluctuations. From *Sanders* [1961].

geoelectric and magnetic fields. Unfortunately this example is the only direct comparison between the geoelectric and magnetic fields that could be found in the literature, and more measurements and analysis (especially recent data obtained using digital equipment) would be important to collect in order to fully characterize the behavior of the geoelectric field relative to the magnetic field after the occurrence of a CME. This can be considered additional future work proposed by the results of this paper.

[24] Instead, the author believes that a more comprehensive (full-vector Maxwell's equations) electrodynamics model is required, one that takes into account the global and transient nature of the ionospheric currents and resulting electromagnetic wave propagation. This model, described below, leads to the possibility of a fourth mechanism that has not yet been proposed or studied: geoelectric field generation due to transient intraionosphere charge displacements.

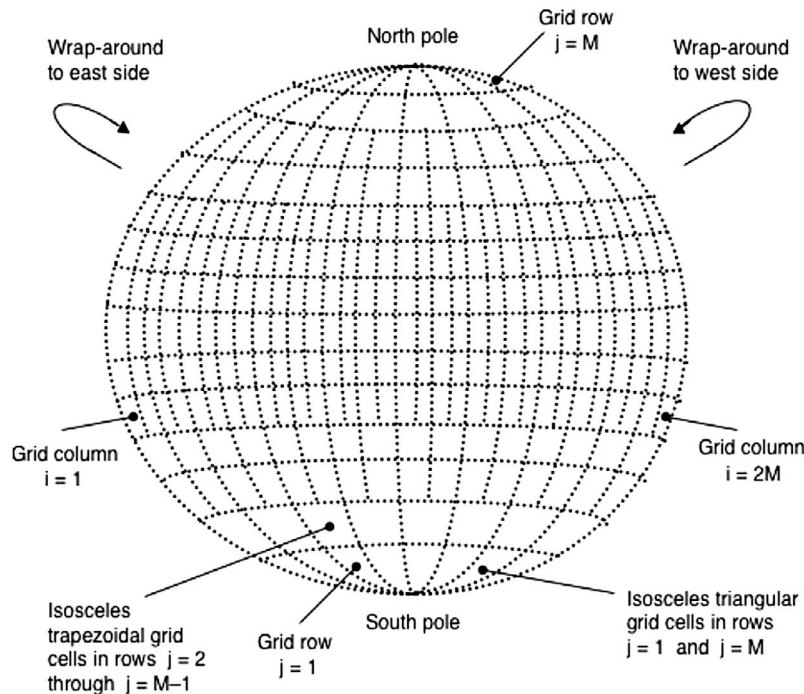


Figure 5. General layout of the 3-D FDTD lattice covering the complete Earth sphere as seen in a TM plane from a constant radial coordinate. Note that this image is not drawn to scale. Each grid cell, regardless of its location near the equator or near the poles, is $\sim 40 \times 40$ km laterally in size. This diagram is drawn to demonstrate the merging of cells in the east-west direction as either pole is approached. The ability for this model to provide isotropic wave propagation (for the free-space case) regardless of the merging of cells and converging cells at the poles is demonstrated in the work of *Simpson and Taflove* [2002].

[25] Specifically, consider the position variability around the poles of the ionospheric currents caused by a CME flowing downward (radially inward), then across the ionosphere at an altitude of ~ 100 km, and upward (radially outward). This spatial variability of the ionospheric currents results in a complex arrangement of charge displacement within the constant altitude plane of ~ 100 km above Earth's surface (as can also be seen through the ionosphere current distribution shown in Figure 6 and will be discussed in section 5). If these lateral charge displacements at an altitude of ~ 100 km happen to be parallel to a power line of a power grid, for example, they can induce large voltages across that line. Further, these variable length lateral ionospheric currents (with length depending on how far they flow over a specific region at ~ 100 km altitude before going vertically upward again) lead to lateral electric fields throughout the ionosphere. The behavior of these fields over time resembles the charging of a capacitor, where the two plates of the capacitor are at ~ 100 km within the ionosphere (and the electric fields extend laterally between them at ~ 100 km altitude). Thus, the ionospheric currents cannot be assumed to be infinite or unrealistically large, as is the case in previous plane wave method models, and the time variation of the surface geoelectric field results of section 5 will be shown (depending on the location of interest and the arrangement of the overlying ionospheric currents) to resemble the charging of a capacitor. Because these transient geoelectric fields at the surface of the Earth result from capacitive effects within the ionosphere, not from induction

processes involving a plane wave incident on the conductive Earth, the plane wave method is simply incapable of accounting for this mechanism. Hence, the time domain, full-vector Maxwell's equations model described in section 4 is employed here to study these effects.

4. Model Description

[26] For the global Earth-ionosphere Maxwell's equations model reported in this study, the annular spherical FDTD space grid first described in the work of *Simpson and Taflove* [2004] is utilized. A global model is employed because at the low-frequency range of interest, the induced electromagnetic waves propagate globally with little attenuation and also penetrate deeply into the lithosphere (even to depths of 400 km for long simulation run times).

[27] Within each constant radius (constant altitude) surface, the FDTD grid is formed by lines of geographic latitude and longitude. The eccentricity of grid cells in the polar regions is mitigated by an adaptive cell-combining technique applied to adjacent grid cells in the east-west direction. This technique permits maintenance of the time step at nearly the level allowed by the Courant stability condition for the square equatorial cells, yielding a greatly improved computational efficiency relative to conventional spherical coordinate FDTD formulations.

[28] Figure 5 illustrates the FDTD space grid as seen at a constant radial coordinate. The transverse magnetic (TM) spherical surface shown is composed of isosceles trapezoidal

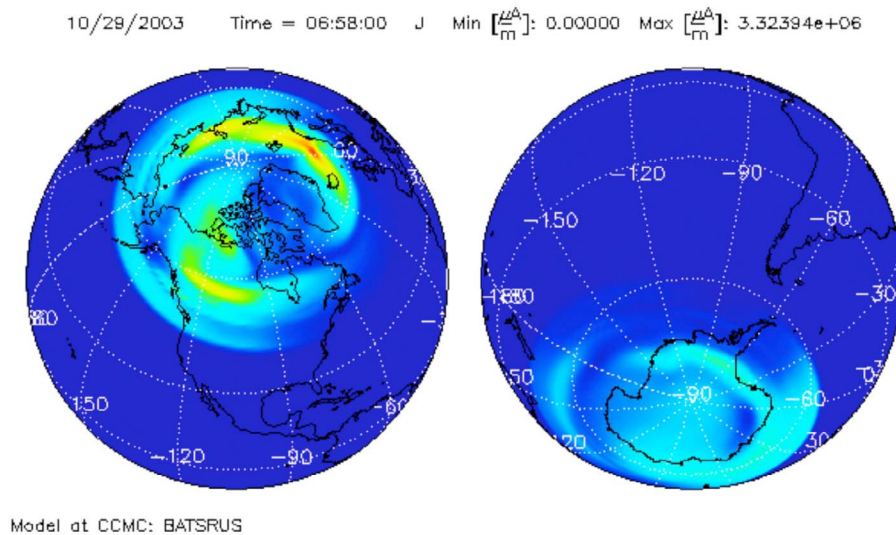


Figure 6. Composite ionospheric current magnitude variation for the region 1 currents only at 06:58 UT on 29 October 2003 during the Halloween storm as calculated by the CCMC BATS-R-US model. Note that the FDTD model accounts for the separate, fully 3-D directional variation of the ionospheric current amplitudes: the north-south, east-west, and radial (vertically up-down) current components.

cells, along with one ring of isosceles triangular cells encircling each pole. The full 3-D space grid consists of alternating TM and transverse electric (TE) field component surfaces that are stacked and coupled in the radial direction. Ampere's and Faraday's Laws in their integral forms are applied to implement leapfrog time stepping relations for the electric (E) and magnetic (H) field vector components within the grid [Simpson and Tafløve, 2004]. An east-west wrap-around (periodic boundary condition) completes each spherical grid surface.

[29] In this study, the annular FDTD space grid extends downward into the lithosphere and upward into the atmosphere/ionosphere around the entire Earth sphere within ± 400 km of sea level. The grid's radial (vertical) spatial resolution is 5 km; its lateral (horizontal) spatial resolution at the equator is $\sim 40 \times 40$ km; and the time step is 3 μ s. For the ionosphere, isotropic conductivity profiles are assigned according to the daytime and nighttime exponential profiles of Bannister [1984]. Topographic and bathymetric data from the NOAA-NGDC "Global Relief CD-ROM" are utilized. In general, lithosphere conductivity values are assigned according to Hermance [1995] depending upon the location of an E field component (i.e., below an ocean or within a continent). However, for Europe and North America, the same conductivity profiles are employed as used previously in regional GIC calculations as discussed in the work of Viljanen *et al.* [2006] for Mäntsälä, Finland, and in the work of Pulkkinen *et al.* [2010] for the North American power transmission system node at a high latitude.

[30] The FDTD models are excited by the disturbed ionospheric currents corresponding to 06:58 UT on 29 October 2003 of the Halloween storm, as obtained from a combination of several MHD-based models used to compute the Sun-to-Earth propagation of CMEs [Pulkkinen *et al.*, 2010]. These data are freely available from the Community Coordinated Modeling Center (CCMC) operated at NASA Goddard Space Flight Center. Specifically, ending with the

BATS-R-US MHD model, fully 3-D high-latitude ionospheric currents are obtained at 1 min time increments. Note that BATS-R-US provides only region 1 currents, but these ionospheric currents are sufficient for the northern latitude locations studied in this paper. North-south and east-west components of the ionospheric currents are modeled at 100 km altitude. Radial ionospheric current components extend upward from 100 km to the outer radial boundary of the model. The laterally position-dependent ionosphere current directions and magnitudes are incorporated as an additive term into the FDTD time stepping relation for the Ampere-Maxwell Law [Tafløve and Hagness, 2005].

[31] It is found, as expected, that the ionospheric currents closest to Earth's surface have the largest impact on the surface electromagnetic fields. Additional simulations which extended the radial boundary of the grid outward by ~ 200 km yielded nearly identical surface fields.

5. Results and Discussion

[32] Now are reported the results of the global FDTD Maxwell's equations model for a hypothetical scenario wherein the ionospheric currents predicted by BATS-R-US at 06:58 UT on 29 October 2003 of the Halloween storm are assumed at each position to increase linearly in time from zero to 10% of their maximum amplitude attained at that position as calculated by BATS-R-US over 1.5 s, and then remain constant. The composite (maximum) amplitude spatial variation of these ionospheric currents is shown in Figure 6. The assumed transient occurs over a time span that is consistent with the most rapid measured fluctuations reported by Hessler and Wescott [1959] and Sanders [1961], as well as in the magnetometer measurements of section 2. The FDTD-computed surface geoelectric and magnetic field time waveforms at Mäntsälä, Finland and at a high-latitude North American power transmission

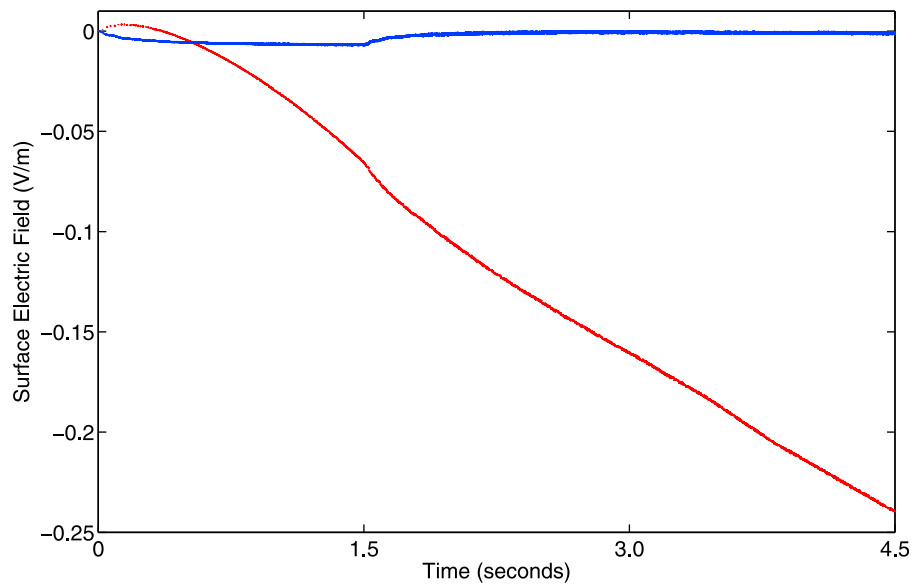


Figure 7. FDTD-computed surface E field at (daytime) Mäntsälä, Finland, resulting from the hypothetical 1.5 s long ionospheric current pulse. The solid blue line corresponds to the east-west E field component, and the dotted red line corresponds to the north-south E field component.

system node were recorded over a total of 1,500,000 time steps, or 4.5 s.

[33] In the above transient ionospheric current scenario, the FDTD-computed time rate of change for the induced northward component surface magnetic field at the North American site, for example, is found to be 119 nT/s. Although this value is not directly comparable to the results of Figures 1 and 2 because the FDTD model corresponds to a different CME scenario, making a general comparison, the FDTD calculated maximum magnetic field time rate of change is seen to be ~ 20 times larger than the maximum time rate of change of the northward component recorded in Greenland as shown in Figures 1 and 2 (corresponding to -5.7 nT/s, if we use the simple linear approximation between 1 s samples which were shown in Figure 2 to provide under sampled data). Comparing these numbers, we must, for example, take into account that the CME occurring in Figures 1 and 2 is small scale and (to the author's knowledge) had no negative impact on any electrotechnical systems. An extreme CME, which is of interest in this paper, would very likely involve much more rapid and extreme changes to the surface magnetic field. As a result, until short-timescale measurements of the geomagnetic field are collected after more extreme CMEs, the time rate of change of the magnetic field of 119 nT/s is not considered impossible. And again, defining realistic time rates of change over short timescales (< 10 s) of the magnetic field after extreme CMEs is considered additional future work proposed by the results of this paper.

[34] Next, Figures 7 and 8 depict the corresponding FDTD-computed time waveforms of the induced horizontal east-west and north-south E fields at the Finland and North American sites. Over the 4.5 s simulation interval, the peak E field amplitudes are 0.24 V/m (240 V/km) and 0.56 V/m (560 V/km). Several comments arise:

[35] 1. The North American E field values are expected to be higher than the Finland values because at 06:58 UT,

daytime conditions existed over Finland, thereby yielding higher ionosphere electron densities and conductivity profiles (and thus more loss) at lower altitudes than for nighttime conditions. Further, the amplitude difference between the north-south and east-west components at each location are due to the direction and position variation of the overlying ionospheric currents. Let us consider the properties of the modeled ionosphere when examining these results. Figure 9 illustrates the assumed daytime and nighttime exponential ionospheric conductivity profiles according to *Bannister* [1984] that are also employed in the FDTD model as mentioned in section 4. Note that these profiles are isotropic, and so do not represent all of the physics of the ionosphere. They were originally developed for calculating the propagation of extremely low-frequency electromagnetic waves in the Earth-ionosphere system (for waves with periods down to about 0.002 s, corresponding to a frequency of ~ 500 Hz) and for altitudes below about 120 km. These profiles are only intended to be used in the very bottom portion of the ionosphere, but here they are just continued to the upper radial boundary of the FDTD grid for simplicity and to provide a smooth transition to the upper perfect electric conductor boundary of the FDTD model where the E fields are set to zero. Since the north-south and east-west direction ionospheric current components are located at an altitude of 100 km, we would not expect much electromagnetic propagation from these ionospheric currents toward the upward (outward radial) direction much past an altitude of about 120 km owing to the exponentially increasing ionospheric conductivity profiles in that direction.

[36] 2. For either location, the computed transient horizontal E field component values of several hundred volts per kilometer would be sufficient to induce transient voltages exceeding 10 kV on overhead power transmission line conductors extending for long distances parallel to these field components. By way of comparison, we note that the E fields computed using the present model are one order of

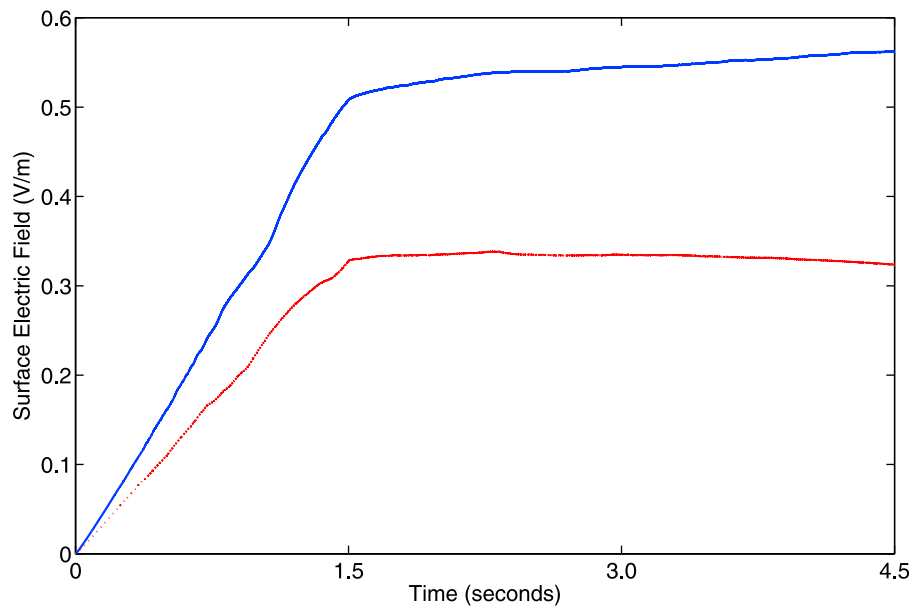


Figure 8. FDTD-computed surface E field at the (nighttime) North American power transmission system node resulting from the hypothetical 1.5 s long ionospheric current pulse. The solid blue line corresponds to the east-west E field component, and the dotted red line corresponds to the north-south E field component.

magnitude higher than the 10–50 V/km values reported in the literature. (For example, *Sanders* [1961, Figure 2] shows an upper bound of 25 V/km in the auroral zone; *Harang* [1951], reported “a minimum of 50 V/km” recorded on one Norwegian wireline during the storm of 24 March

1940.) This is primarily due to the order (1 s) characteristic fluctuation time assumed here for the ionospheric current. Additional short-timescale measurements would be needed to fully characterize the transient voltages induced on power lines.

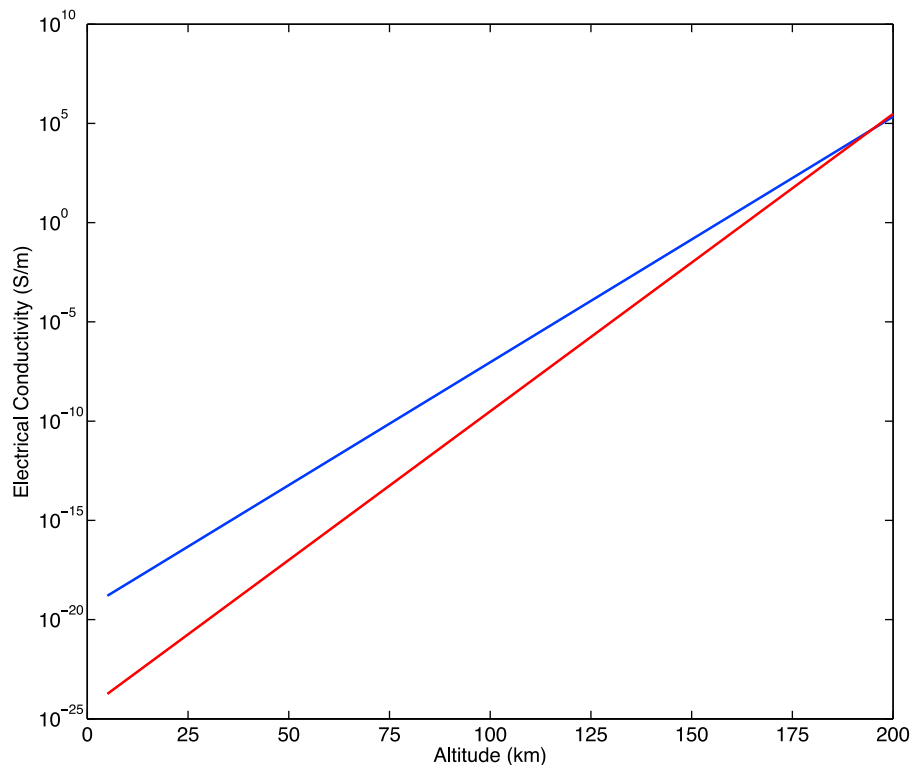


Figure 9. Variation in the FDTD model of the daytime and nighttime ionospheric conductivity profiles with altitude.

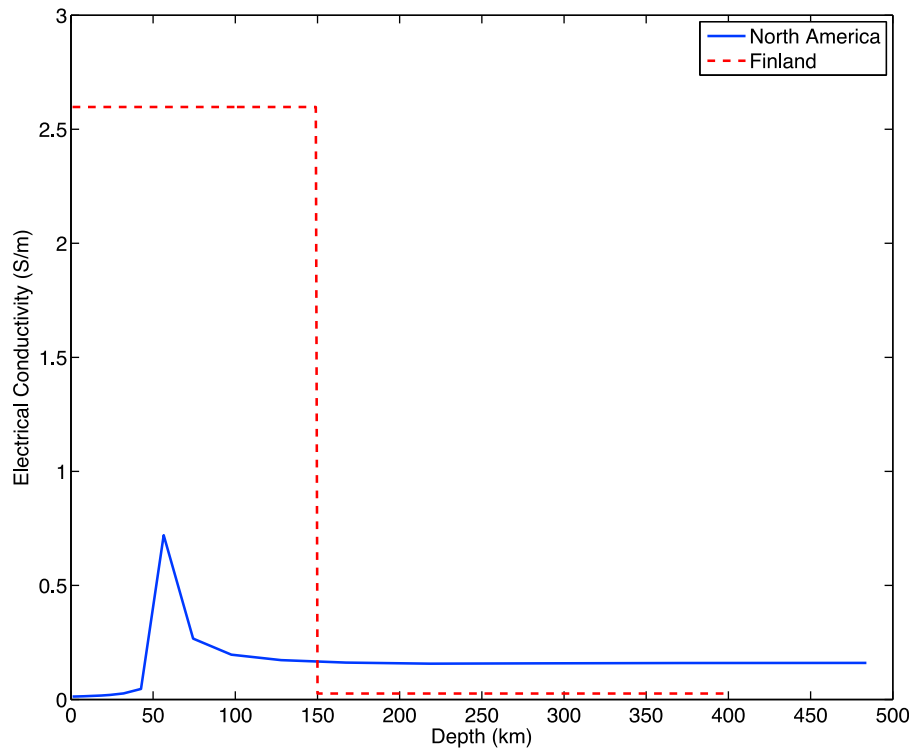


Figure 10. Variation in the FDTD model of the ground conductivity profiles with depth for North America and Europe (the Finnish ground conductivity values are modeled throughout Europe).

[37] 3. The continued nearly linear ramping of the north-south E field component in Figure 7, even after the assumed leveling-off of the ionospheric current amplitude at 1.5 s, suggests an accumulating intraionosphere charge displacement in the vicinity of Finland, similar to the charging of a capacitor. Interestingly, this phenomenon was not observed for the North American site, where both horizontal E field components remained essentially constant after 1.5 s, in a manner consistent with the assumed constancy of the ionospheric current during that time.

[38] 4. Following up on the previous point, transient ionospheric currents leading to momentary intraionosphere charge displacements have been previously observed in the context of the nuclear electromagnetic pulse (NEMP) phenomenon [Longmire, 1978]. However, the NEMP involves extremely rapid transient radial movements of charge from a central position (i.e., a high-altitude nuclear explosion) rather than what appears to be much slower longitudinal movements of charge due to fluctuating CME-originated ionospheric currents.

[39] 5. Additional simulations involving the same short-time ionospheric current sources indicate that the lithosphere conductivity has little impact on the induced transient surface E fields. Specifically, Figure 10 illustrates the assumed ground conductivity variation with depth in the FDTD model for Europe and North America. As mentioned in section 4, these are the same conductivity profiles employed previously for regional GIC calculations as discussed in the work of Viljanen *et al.* [2006] for Mäntsälä, Finland, and in the work of Pulkkinen *et al.* [2010] for the North American power transmission system node at a high latitude. In a

separate, additional FDTD simulation wherein the assumed ground conductivity profiles for Europe and North America are exchanged (so that the Europe ground conductivity profile is used for North America and vice versa), the transient surface E fields are found to be nearly identical to those of Figures 7 and 8 (the results of the unexchanged ground conductivity case). This is quite unlike the previously analyzed magnetic field coupling mechanisms for the induction of GICs, but would be expected for the transient E fields generated by short-time (impulsive) charge displacements within the ionosphere. This is because the long-time surface electromagnetic fields relating to the GICs are impacted by the slow diffusion of electromagnetic energy through the conductive Earth, leading to temporal integration and involving time spans of even minutes. As such, the ground conductivity layering down to even 400 km affects the surface electromagnetic fields over these longer time spans. However, the surface E field variations studied here, which are transient and on the order of 1 s, are not yet influenced by the diffused energy through the conductive Earth and are instead primarily impacted by the ionospheric currents located overhead.

[40] Note that the FDTD model solves the complete Maxwell's equations, and can thus also be used in a straightforward manner for the long-time GIC calculations wherein the ground conductivity would be seen to impact the results. Considering present supercomputing capabilities, however, the plane wave method, image method, or other similar techniques are more feasible for GIC studies, since the time step of the FDTD model is on the order of 3 μ s. Time stepping the FDTD model out to 10 s, for

example, would require 3 million time steps, or about 96 h of simulation time on 64 processors.

6. Future Work

[41] In 2010, the research group of the author published a 3 D, Cartesian coordinate FDTD magnetized ionospheric plasma algorithm [Yu and Simpson, 2010a]. This algorithm has recently been adapted to the general 3-D global FDTD models utilized for the studies of this paper, thereby upgrading the isotropic exponential conductivity ionosphere profiles to a fully anisotropic ionospheric plasma that accounts for the complete geomagnetic field. This newly advanced global FDTD model has been completed and validated [Yu and Simpson, 2010b]. As part of future work, the effect of the magnetized ionospheric plasma on the surface E fields during space weather events will be investigated. This modeling will require details of the background geomagnetic field, which has been omitted from the present study because the isotropic ionosphere used in the model of this paper is not affected by the geomagnetic field (which would make it anisotropic). The only magnetic fields calculated or utilized in the present model are those induced by the ionospheric currents.

[42] As such, considering the smooth variation of the curves in Figure 9, the 5 km radial (vertical) resolution of the model is currently sufficient for modeling the isotropic ionospheric conductivity variations (also, note that this model at its current resolution has been previously validated for its calculated propagation attenuation versus frequencies below 500 Hz) [Simpson and Taflove, 2004]. But later, as the magnetized ionospheric plasma is accounted for, not only will the geomagnetic field data be included, but also the ionospheric particle density and collision frequency variations with altitude and position around Earth. Thus, the resolution of the FDTD model will be increased as needed to sufficiently account for the variations of these parameters with position.

[43] As part of other future work, note that the present FDTD model assumes a constant (with respect to time, not space) and isotropic ground conductivity regardless of the frequency of the impinging electromagnetic wave. This is the same as for the model used in the propagation attenuation validation study of Simpson and Taflove [2004]. Algorithms already exist that accommodate the frequency dependence of material parameters in FDTD models [Taflove and Hagness, 2005], and these could be introduced along with the anisotropy into the lithosphere region of the global FDTD model in the future to provide even more realistic calculations when such details are available for the underlying rock structures.

7. Summary and Conclusions

[44] This paper has reported the first three-dimensional, full-vector time domain Maxwell's equations model of the global Earth-ionosphere system for computing the surface electromagnetic fields generated by the impact of a coronal mass ejection. Assuming order(1 s) ionospheric current fluctuations during this event, momentary intraionosphere charge displacements are created that generate significant transient horizontal geoelectric fields at Earth's surface.

Following a severe CME, such E fields can exceed 100 V/km and induce transient voltages exceeding 10 kV on long parallel overhead power transmission lines.

[45] It is proposed that measurements be conducted to characterize short-time ionospheric current fluctuations, and to determine what hazards, if any, are posed to power grids by such fluctuations.

[46] As part of future work, the effect of the anisotropic, magnetized ionospheric plasma on the surface electromagnetic fields during space weather events will be studied using FDTD global models [Yu and Simpson, 2010b]. This work will build on the results of this paper, and will provide an even more comprehensive analysis than that possible using the previously employed techniques involving, for example, complex image theory and the plane wave method.

[47] Also, as part of future work, additional ionospheric current systems (region 2 and other equatorial currents systems) will be incorporated into the FDTD models. These additions will complement the truly global nature of the FDTD grids, and will permit studies of electromagnetic fields at any location around Earth, not just at the northern latitude locations as recorded in this paper.

[48] **Acknowledgments.** This work is supported by National Science Foundation CAREER Award grant 0955404. Supercomputing resources are provided by the University of New Mexico's Center for Advanced Research Computing and the New Mexico Computing Applications Center. The author is grateful to Claudia Stolle of the National Space Institute at the Technical University of Denmark for providing the magnetic field measurement data for Figures 1 and 2 and to Jurgen Watermann for helping the author connect with Claudia Stolle. The author is also grateful to Antti Pulkkinen of Catholic University of America at NASA/GSFC for very useful discussions and for providing Earth's conductivity profile for the North American high-latitude power transmission system node.

[49] Robert Lysak thanks the reviewers for their assistance in evaluating this paper.

References

- Bannister, P. (1984), ELF propagation update, *IEEE J. Oceanic Eng.*, *0E-9*, 179–188.
- Bannister, P. (1985), The determination of representative ionospheric conductivity parameters for ELF propagation in the Earth-ionosphere waveguide, *Radio Sci.*, *20*, 977–984, doi:10.1029/RS020i004p00977.
- Bolduc, L. (2002), GIC observations and studies in the Hydro-Quebec power system, *J. Atmos. Sol. Terr. Phys.*, *64*, 1793–1802, doi:10.1016/S1364-6826(02)00128-1.
- Harang, L. (1951), *The Aurorae*, pp. 105–106, Chapman and Hall, London.
- Hernance, J. (1995), Electrical conductivity of the crust and mantle, in *Global Earth Physics: A Handbook of Physical Constants*, edited by T. J. Ahrens, pp. 190–205, AGU, Washington, D. C.
- Hessler, V. P., and E. M. Wescott (1959), Rapid fluctuations in Earth currents at College, *Rep. AFCRC-TN-59-275*, *ASTIA Doc. AD214418*, Geophys. Inst., Univ. of Alaska, Fairbanks.
- Kappenman, J. G. (2005), An overview of the impulsive geomagnetic field disturbances and power grid impacts associated with the violent Sun-Earth connection events of 29–31 October 2003 and a comparative evaluation with other contemporary storms, *Space Weather*, *3*, S08C01, doi:10.1029/2004SW000128.
- Kappenman, J. G. (2006), Great geomagnetic storms and extreme impulsive geomagnetic field disturbance events—An analysis of observational evidence including the great storm of May 1921, *Adv. Space Res.*, *38*, 188–199, doi:10.1016/j.asr.2005.08.055.
- Kappenman, J. G., L. J. Zanetti, and W. A. Radasky (1997), Geomagnetic storms can threaten electric power grid, *Earth Space*, *9*, 9–11.
- Kotobi, A., A. Pulkkinen, and J. J. Simpson (2011), Global FDTD modeling of the Earth-ionosphere system during the 2003 Halloween storms, paper presented at National Radio Science Meeting, U.S. Natl. Comm. for Int. Union Radio Sci., Boulder, Colo.
- Leshner, R. L., J. W. Porter, and R. T. Byerly (1994), SUNBURST—A network of GIC monitoring systems, *IEEE Trans. Power Delivery*, *9*, 128–137, doi:10.1109/61.277687.

- Longmire, C. (1978), On the electromagnetic pulse produced by nuclear explosions, *IEEE Trans. Antennas Propag.*, 26, 3–13, doi:10.1109/TAP.1978.1141796.
- National Research Council of the National Academies (2008), Severe space weather events—Understanding societal and economic impacts, *Workshop Rep.*, Washington, D. C.
- Pulkkinen, A., A. Viljanen, and R. Pirjola (2006), Estimation of geomagnetically induced current levels from different input data, *Space Weather*, 4, S08005, doi:10.1029/2006SW000229.
- Pulkkinen, A., M. Hesse, M. Kuznetsova, and L. Rastatter (2007), First principles modeling of geomagnetically induced electromagnetic fields and currents from upstream solar wind to the surface of the Earth, *Ann. Geophys.*, 25, 881–893, doi:10.5194/angeo-25-881-2007.
- Pulkkinen, A., M. Hesse, S. Hbib, L. Van der Zel, B. Damsky, F. Policelli, D. Fugate, W. Jacobs, and E. Creamer (2010), Solar shield: Forecasting and mitigating space weather effects on high-voltage power transmission systems, *Nat. Hazards*, 53, 333–345, doi:10.1007/s11069-009-9432-x.
- Raeder, J., R. L. McPherron, L. A. Frank, S. Kokubun, G. Lu, T. Mukai, W. R. Paterson, J. B. Sigwarth, H. J. Singer, and J. A. Slavin (2001), Global simulation of the geospace environment modeling substorm challenge event, *J. Geophys. Res.*, 106, 381–395, doi:10.1029/2000JA000605.
- Sanders, R. (1961), Effects of terrestrial electromagnetic storms on wireline communications, *IRE Trans. Commun. Syst.*, 9, 367–377, doi:10.1109/TCOM.1961.1097724.
- Shao, X., P. N. Guzdar, G. M. Milikh, K. Papadopoulos, C. C. Goodrich, A. Sharma, M. J. Wiltberger, and J. G. Lyon (2002), Comparing ground magnetic field perturbations from global MHD simulations with magnetometer data for the 10 January 1997 magnetic storm event, *J. Geophys. Res.*, 107(A8), 1177, doi:10.1029/2000JA000445.
- Shepherd, S. G., and F. Shubitidze (2003), Method of auxiliary sources for calculating the magnetic and electric fields induced in a layered Earth, *J. Atmos. Sol. Terr. Phys.*, 65, 1151–1160, doi:10.1016/S1364-6826(03)00159-7.
- Simpson, J. J. (2009), Current and future applications of 3-D global Earth-ionosphere models based on the full-vector Maxwell's equations FDTD method, *Surv. Geophys.*, 30, 105–130, doi:10.1007/s10712-009-9063-5.
- Simpson, J. J., and A. Taflove (2002), Two-dimensional FDTD model of antipodal ELF propagation and Schumann resonance of the Earth, *IEEE Antennas Wireless Propag. Lett.*, 1, 53–56, doi:10.1109/LAWP.2002.805123.
- Simpson, J. J., and A. Taflove (2004), Three-dimensional FDTD modeling of impulsive ELF antipodal propagation and Schumann resonance of the Earth-sphere, *IEEE Trans. Antennas Propag.*, 52, 443–451, doi:10.1109/TAP.2004.823953.
- Simpson, J. J., and A. Taflove (2005), Electrokinetic effect of the Loma Prieta earthquake calculated by an entire-Earth FDTD solution of Maxwell's equations, *Geophys. Res. Lett.*, 32, L09302, doi:10.1029/2005GL022601.
- Simpson, J. J., and A. Taflove (2006a), ELF radar system proposed for localized D region ionospheric anomalies, *IEEE Geosci. Remote Sens. Lett.*, 3, 500–503, doi:10.1109/LGRS.2006.878443.
- Simpson, J. J., and A. Taflove (2006b), A novel ELF radar for major oil deposits, *IEEE Trans. Geosci. Remote Sens. Lett.*, 3, 36–39, doi:10.1109/LGRS.2005.856118.
- Simpson, J. J., and A. Taflove (2007), A review of progress in FDTD Maxwell's equations modeling of impulsive sub-ionospheric propagation below 300 kHz, *IEEE Trans. Antennas Propag.*, 55, 1582–1590.
- Taflove, A., and S. C. Hagness (2005), *Computational Electrodynamics: The Finite-Difference Time-Domain Method*, 3rd ed., 1006 pp., Artech House, Norwood, Mass.
- Viljanen, A., A. Pulkkinen, R. Pirjola, K. Pajunpää, P. Posio, and A. Koistinen (2006), Recordings of geomagnetically induced currents and a nowcasting service of the Finnish natural gas pipeline system, *Space Weather*, 4, S10004, doi:10.1029/2006SW000234.
- Yu, Y., and J. J. Simpson (2010a), An E-J collocated 3-D FDTD model of electromagnetic wave propagation in magnetized cold plasma, *IEEE Trans. Antennas Propag.*, 58, 469–478, doi:10.1109/TAP.2009.2037706.
- Yu, Y., and J. J. Simpson (2010b), Global FDTD modeling of electromagnetic wave propagation within the Earth-ionosphere system including a magnetized cold plasma ionosphere, paper presented at National Radio Science Meeting, U.S. Natl. Comm. for Int. Union Radio Sci., Toronto, Ont., Canada.

J. J. Simpson, Electrical and Computer Engineering Department, University of New Mexico, MSC01 1100, 1 University of New Mexico, Albuquerque, NM 87131, USA. (simpson@ece.unm.edu)